

Study of the Radio-Frequency Size Effect in Potassium

P. S. PEERCY, W. M. WALSH, JR., L. W. RUPP, JR., AND P. H. SCHMIDT
Bell Telephone Laboratories, Murray Hill, New Jersey

(Received 19 February 1968)

An initial study of the radio-frequency size effect (RFSE) in potassium by Koch and Wagner revealed several interesting features which occurred on tilting the magnetic field out of the sample plane. We wish to report an independent investigation and interpretation of the RFSE in potassium. Because of increased sample purity and higher experimental frequencies (up to 35 MHz), a number of new features of the phenomenon have been observed in addition to the primary RFSE series. These new signals occur in the low-field range where sharply resolved signals are observed. The higher-field regime where oscillatory signals are observed has also been studied in detail. For exciting currents polarized perpendicular to the magnetic field, these oscillatory signals are observed to exhibit a cutoff which is a strong function of tilt. On the basis of these experiments, a geometrical model of the RFSE is proposed which differs significantly from that used by Koch and Wagner. The model successfully accounts for the tilt dependence of both the primary RFSE series and the newly resolved signals. Using currents polarized parallel to the magnetic field, signals were observed due to the transition from effective to ineffective electrons spanning the sample thickness. This transition occurs for electrons near the limiting point of the Fermi surface and provides a caliper for the orbits in this region. Studies of these orbits confirm the observation of Koch and Wagner that the Fermi surface is indeed spherical and not distorted in the vicinity of the limiting points by either a spin-density or a charge-density wave.

IN 1962 Gantmakher¹ discovered well-defined changes in the 3–5-MHz surface inductance of thin plates of pure tin at liquid-helium temperatures as a function of a magnetic field applied parallel to the sample surface. The impedance anomalies occurred at field values such that cyclotron orbits of extremal dimensions normal to the sample surface carried rf currents from one skin layer to the other. The fractional widths of the signals were of the order of the ratio of the skin depth to the sample thickness, typically $\sim 10^{-2}$. This radio-frequency size effect (RFSE) is an excellent means of directly caliper extremal dimensions of Fermi surfaces of pure metals. When generalized to include arbitrary orientation of the magnetic field relative to the sample plane, it is also a transport phenomenon of considerable intrinsic interest. The latter aspect of the RFSE is difficult to interpret in most metals due to the geometrical complexities of their Fermi surfaces. The alkali metal potassium, however, is known to have a single-sheeted and essentially spherical Fermi surface, and therefore offers an excellent opportunity to examine the intricacies of the RFSE in detail.

An initial study of the RFSE in potassium has been reported by Koch and Wagner² (KW) who noted several interesting features which result from tilting the magnetic field relative to the sample plane and from changes in the polarization of the incident radiation relative to the magnetic field. The present paper summarizes an independent investigation and interpretation of the RFSE in potassium. Because of increased sample purity and the use of higher experimental frequencies a number of new features of the phenomenon have been observed in the low-magnetic-field range where sharply resolved signals are observed. The higher-field range

where oscillatory signals occur has also been studied in some detail. The spectroscopic aspects of the data, i.e., signal position variation with tilt angle, are consistent with the predictions of a geometrical model which differs significantly from that of Koch and Wagner.²

In an effort to clarify the relationships between earlier treatments of the RFSE and to introduce various concepts entering our own interpretation, Sec. I contains a brief history of the field. An extensive review has recently been given by Gantmakher.³ Following a description of the experimental details (Sec. II) the general features of the potassium data are outlined (Sec. III) and the model is then presented (Sec. IV). Quantitative comparison of theory and experiment is made in Sec. V.

I. INTRODUCTION

An electromagnetic wave incident on the surface of a conductor is nearly totally reflected if its angular frequency ω is less than the plasma frequency ω_p of the mobile charge carriers ($\omega_p = 4\pi ne^2/m^* \sim 10^{16}$ rad/sec for a carrier density $n \sim 10^{22}$ cm⁻³ and effective mass $m^* \sim m_0$; m_0 is the free-electron mass). The incident radiation produces a surface current layer (skin effect) of thickness δ which is $\sim 10^{-4}$ cm in pure metals at low temperatures. In very pure metals at liquid-helium temperatures the carrier mean free path between collisions l may be $\sim 10^{-2}$ cm, i.e., $l \gg \delta$. The skin depth is then independent of l and is referred to as "anomalous."⁴ Under these conditions the screening currents are carried primarily by those conduction electrons which are moving parallel to the surface within the skin depth. These electrons with small velocities normal to the surface are known as effective electrons.

¹ V. F. Gantmakher, in *Progress in Low-Temperature Physics*, edited by C. J. Gorter (North-Holland Publishing Co., Amsterdam, 1967), p. 181.

⁴ G. E. H. Reuter and E. H. Sondheimer, *Proc. Roy. Soc. (London)* **A195**, 336 (1948). For a review article see A. B. Pippard, *Advan. Electron. Electron Phys.* **6**, 1 (1954).

¹ V. F. Gantmakher, *Zh. Eksperim. i Teor. Fiz.* **42**, 1416 (1962); **43**, 345 (1962); **44**, 811 (1963) [English transl.: *Soviet Phys.—JETP* **15**, 982 (1962); **16**, 247 (1962); **17**, 549 (1963)].

² J. F. Koch and T. K. Wagner, *Phys. Rev.* **151**, 467 (1966).

Under anomalous skin effect (ASE) conditions enhanced penetration of the rf currents into the bulk of the metal can be produced by application of a magnetic field H which causes effective electrons to spiral into the metal along their cyclotron orbits. The magnetic-field-induced variations of a metal's surface impedance observed in the RFSE experiments result from interactions of this bulk current distribution with the opposite surface of the specimen. For an appreciable number of electrons to complete at least half a cyclotron orbit the mean free path must be comparable to or greater than an orbit diameter D ($l \gtrsim D$) or, equivalently, the condition $\omega_c \tau \gtrsim 1$ must be satisfied, where $\omega_c = eH/m^*c$ is the angular frequency of the cyclotron motion and τ is the mean scattering time.

Shortly after Azbel' and Kaner⁵ presented their theory of cyclotron resonance under ASE conditions ($\omega = n\omega_c$, $\omega\tau \gg 1$, H parallel to the sample surface), Kaner⁶ discussed possible effects of finite sample thickness. In particular he pointed out that at sufficiently low magnetic fields the orbits of the resonant electrons would become larger than the sample thickness L and collisions of the charge carriers with the surface would cause the series of subharmonic resonances to cut off. Such truncations were later observed by Khaikin⁷ and have been exploited to yield both extremal effective masses and orbit dimensions. For the cutoff to be well defined one must have $\omega_c \tau \gg 1$ and the spread in orbit diameters normal to the sample surface ΔD over the band of resonant electrons must be small compared to the typical orbit dimension.

Azbel⁸ pointed out that such groups of resonant electrons carry currents into the metal in a way which can create an image of the surface current layer one orbit diameter below the surface. The electric fields associated with these image currents ("field splashes") can in turn accelerate other electrons and thus propagate a series of field splashes into the metal. Such multi-layered propagation effects also require that the band of resonant electrons have a small spread in orbit dimension normal to the sample surface (ideally $\Delta D \lesssim \delta$). Neither the resonance cutoff nor well-defined field splashes can exist, for example, in potassium whose essentially spherical Fermi surface⁹ ($k_F = 0.744 \times 10^8 \text{ cm}^{-1}$) and isotropic effective mass¹⁰ ($m^*/m_0 = 1.21$) cause all electrons to resonate simultaneously with a distribution of orbit diameters from zero at the limiting

point of the distribution up to $D_0 = 2\hbar c k_F / eH = (9.79 \text{ cm G})/H$ for the stationary belly orbit.

Kaner¹¹ later proposed that by slightly tilting the magnetic field out of the sample plane one should be able to preferentially select electrons in stationary orbits (closed orbits in real space) since the remaining electrons would spiral along the field and either collide with the surface or drift into the metal. The stationary-orbit electrons would be expected to define a very narrow band on the Fermi surface and thus a small range of orbit diameters which would carry enhanced currents at resonance.

In view of Gantmakher's discoveries¹ Kaner¹¹ extended the concept of field splashes and orbit cutoff to the low-frequency regime ($\omega \ll \omega_c$, $\omega_c \tau \gg 1$). Under these conditions the stationary-orbit electron can interact $\omega_c \tau$ times with the surface currents whose phase is effectively constant during a scattering time ($\omega\tau \ll 1$). When $\omega\tau \ll 1$ the precise value of the experimental frequency is important only in determining a skin depth but significant changes in surface impedance may occur in finite samples if field splashes exist. The model Kaner proposed implies that the conductivity and surface impedance anomalies would be dominated by electrons which make multiple passes through the skin depth in the tilted field geometry.

Subsequently Gantmakher and Kaner¹² showed that in the tilted field geometry, field splashes could be produced by nonstationary orbit electrons which are accelerated by a single passage through the skin layer and then spiral into the metal along the magnetic field. It will become apparent that the ability of drifting electrons to carry currents into the bulk of the metal is the dominant feature of the RFSE experiments in potassium. Gantmakher and Kaner¹³ have also reported sinusoidal size-effect oscillations in the surface impedance of tin plates with the magnetic field nearly normal to the sample. In this case currents are carried into the metal by ineffective electrons (those having finite velocities normal to the surface at all points on their cyclotron trajectories). This effect is similar to Sondheimer's earlier prediction of a weakly oscillatory variation of the transverse dc magnetoresistance of thin metal plates.¹⁴ The effect is considerably enhanced at radio frequencies by the existence of a skin effect.

Despite considerable development of the ability to interpret many aspects of the RFSE data, the subject remains highly empirical. Since no general solution of the boundary-value problem for an arbitrary Fermi surface in the presence of a magnetic field exists,

⁵ M. Ya. Azbel' and E. A. Kaner, Zh. Eksperim. i Teor. Fiz. **32**, 896 (1957) [English transl.: Soviet Phys.—JETP **5**, 730 (1957)].

⁶ E. A. Kaner, Dokl. Akad. Nauk SSSR **119**, 471 (1958) [English transl.: Soviet Phys.—Doklady **3**, 314 (1958)].

⁷ M. S. Khaikin, Zh. Eksperim. i Teor. Fiz. **41**, 1773 (1961); **43**, 66 (1962) [English transl.: Soviet Phys.—JETP **14**, 1260 (1962); **16**, 42 (1963)].

⁸ M. Ya. Azbel', Zh. Eksperim. i Teor. Fiz. **39**, 400 (1960) [English transl.: Soviet Phys.—JETP **12**, 283 (1961)].

⁹ D. Shoenberg and P. J. Stiles, Proc. Roy. Soc. (London) **A281**, 62 (1964).

¹⁰ C. C. Grimes and A. F. Kip, Phys. Rev. **132**, 1991 (1963).

¹¹ E. A. Kaner, Zh. Eksperim. i Teor. Fiz. **44**, 1036 (1963) [English transl.: Soviet Phys.—JETP **17**, 700 (1963)].

¹² V. F. Gantmakher and E. A. Kaner, Zh. Eksperim. i Teor. Fiz. **45**, 1430 (1963) [English transl.: Soviet Phys.—JETP **18**, 988 (1964)].

¹³ V. F. Gantmakher and E. A. Kaner, Zh. Eksperim. i Teor. Fiz. **48**, 1572 (1965) [English transl.: Soviet Phys.—JETP **21**, 1053 (1965)].

¹⁴ E. H. Sondheimer, Phys. Rev. **80**, 400 (1950).

particularly if H is tilted relative to the sample's surface, considerable ingenuity is required to understand the myriad observable RFSE anomalies. If the magnetic field is confined to the sample plane, however, one can usually interpret the sharp fundamental signals resulting from single extremal orbit dimensions spanning the sample thickness. Such spectroscopic investigations of Fermi surface extremal dimensions have been performed for several metals: tin,¹ indium,¹⁵ tungsten,¹⁶ gallium,¹⁷ aluminum,¹⁸ and cadmium.¹⁹ In this role the RFSE is a very useful tool, complementary in many ways to the more traditional techniques for characterizing the electronic structure of metals. The accuracy with which caliper dimensions may be determined is typically limited to the 1 or 2% range due to the inability to analyze the line shape in detail.

An attempt to solve the line-shape problem has been made by Kaner and Fal'ko²⁰ for the case of a spherical Fermi surface. They calculate the surface impedance in the vicinity of the fundamental RFSE signal for a sample subject to radiation on one surface only and assume that, under high $\omega_c\tau$ and diffuse scattering conditions, it is sufficient to account for loss of the effective electrons due to collisions with the far surface as the field is varied through the range where belly orbits span the sample. Wagner and Koch²¹ have recently performed the corresponding experiment in potassium and have computed both surface resistance and surface reactance variations using the Kaner-Fal'ko formalism. While they report rough agreement between theory and experiment the discrepancies are large enough to indicate that serious approximations have been made, e.g., neglect of radiation from the second surface. In any case, the experiments are usually performed using two-sided excitation, which yields much narrower and far more intense signals whose shapes are quite different from those obtained with unilateral excitation. It is therefore clear that interpretation of the RFSE must remain primarily empirical at this state of development.

¹⁵ V. F. Gantmakher and I. P. Krylov, *Zh. Eksperim. i Teor. Fiz.* **49**, 1054 (1965) [English transl.: *Soviet Phys.—JETP* **22**, 734 (1966)].

¹⁶ W. M. Walsh, Jr., C. C. Grimes, G. Adams, and L. W. Rupp, Jr., in *Proceedings of the Ninth International Conference on Low-Temperature Physics, Columbus, Ohio*, edited by J. A. Daunt *et al.* (Plenum Press, Inc., New York, 1965), p. 765; W. M. Walsh, Jr. and C. C. Grimes, *Phys. Rev. Letters* **13**, 523 (1964).

¹⁷ D. M. Sparlin and D. S. Schreiber, in *Proceedings of the Ninth International Conference of Low-Temperature Physics, Columbus, Ohio*, edited by J. A. Daunt *et al.* (Plenum Press, Inc., New York, 1965), p. 823; J. F. Cochran and C. A. Shiffman, *Phys. Rev.* **140**, A1678 (1965); A. Fukumoto and M. W. P. Strandberg, *Phys. Rev.* **155**, 685 (1967).

¹⁸ J. F. Koch and T. K. Wagner, *Bull. Am. Phys. Soc.* **11**, 170 (1966).

¹⁹ V. P. Naberezhnykh and A. A. Maryakhin, *Phys. Status Solidi* **20**, 737 (1967); R. G. Goodrich and R. C. Jones, *Phys. Rev.* **155**, 745 (1967).

²⁰ E. A. Kaner and V. L. Fal'ko, *Zh. Eksperim. i Teor. Fiz.* **51**, 586 (1966) [English transl.: *Soviet Phys.—JETP* **24**, 392 (1967)].

²¹ T. K. Wagner and J. F. Koch, *Phys. Rev.* **165**, 885 (1968).

II. EXPERIMENTAL CONSIDERATIONS

Potassium samples were prepared in the form of plane-parallel sheets of thickness $L \sim 0.1$ mm by rolling out the vacuum-distilled metal between two layers of Parafilm,²² a soft inert protective material, under degassed mineral oil. No attempt was made to isolate single-crystal regions of the recrystallized sheet in view of the known isotropy of the potassium Fermi surface.⁹ Rectangular samples, 2×1 cm, cut from the sheet were placed between flat glass plates for further protection. The complete sandwich was then inserted in a rectangular coil which served as the tank-circuit inductance of a marginal oscillator. The sample-coil assembly was mounted in a cryostat at the lower end of a 1-m balanced line with the remainder of the oscillator circuitry at the Dewar head. The sample-coil plane was vertical in order that the rotatable horizontal magnetic field H could be directed at an arbitrary angle with respect to the sample surface. By appropriate mounting the linearly polarized currents J induced in the sample surface could be made either vertical ($\mathbf{J} \perp \mathbf{H}$ polarization) or horizontal [$\mathbf{J} \parallel \mathbf{H}$ polarization; in fact $\mathbf{J} \parallel$ (projection of \mathbf{H} in the sample plane)]. A voltage proportional to the field derivative of the sample's surface resistance (dR/dH) was obtained by audio-frequency modulation of the applied field (~ 10 G peak to peak at 165 Hz) and synchronous second detection of the oscillator level. The dependence of dR/dH on H was plotted using an X - Y recorder.

These arrangements are essentially equivalent to those employed by Koch and Wagner, though they also recorded variations in their samples' surface inductance by monitoring the oscillator frequency. The important experimental differences lie in our higher operating frequency, typically ~ 35 MHz in our case versus 0.06 to 2.5 MHz in KW, and in the higher purity of the potassium metal, l being $\sim 4 \times 10^{-2}$ cm at 1.3°K in our material versus $l \sim 6 \times 10^{-3}$ cm for KW. The combination of reduced fractional linewidths ($\Delta H/H \sim \delta/d\alpha\omega^{-1/3}$) and increased signal intensities [$\alpha \exp(-d/l)$] leads to an over-all increase in resolution which permits a more precise comparison of theory with experiment.

III. GENERAL FEATURES OF THE RFSE IN POTASSIUM

Since potassium has an essentially spherical Fermi surface the drifting electrons follow simple helices with each helix axis parallel to \mathbf{H} . When \mathbf{H} is in the sample plane the stationary electrons, whose orbits have maximum diameter, go deeper into the metal than any drifting electrons and produce the primary series of RFSE signals for the $\mathbf{J} \perp \mathbf{H}$ polarization. The series is produced by electrons reexcited in current sheets in the metal and the resulting signals are periodic in H with a period directly proportional to the extremal orbit diameter. The series decreases rapidly in amplitude with

²² "Parafilm," American Can Co.

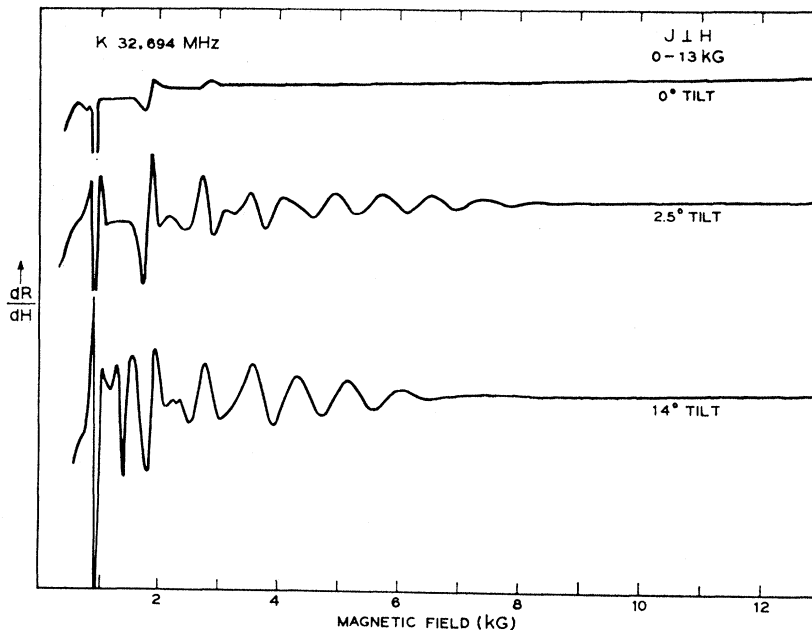


FIG. 1. Data taken on a 0.116-mm sample of potassium at a temperature of 1.4°K with rf currents at a frequency of 32.694 MHz perpendicular to the magnetic field. The upper trace is the signal observed when \mathbf{H} is accurately in the plane of the sample. The center trace, taken with \mathbf{H} tilted 2.5° out of the sample plane, shows the increased amplitude of the higher-order signals as well as the nearly sinusoidal variations occurring at higher fields. The lower trace, taken at 14° tilt, illustrates the "extra" signals which occur on tilting the field out of the sample plane.

increasing magnetic field, only four or five anomalies being observable when \mathbf{H} is accurately parallel to the surface of a flat specimen. The experiments reported by KW demonstrated that the field value to be taken for the extremal-orbit diameter just spanning the sample was the low-field edge of the fundamental RFSE signal. They also noted that the linewidth of the fundamental signal varied as $\omega^{-1/3}$ as expected under ASE conditions.

When the magnetic field is tilted out of the sample plane, the fundamental size-effect series moves slowly to increasing field with increasing tilt angle and the higher-order RFSE anomalies increase significantly in amplitude. The direction of this shift is opposite to that expected on the basis of Kaner's original assumption that stationary orbits dominate the bulk current distribution. KW attributed the shift of the signal to increasing field with increasing tilt angle to drifting electrons and found that for tilt angles up to $\sim 20^\circ$ the data followed a curve of the form $\mathbf{H} = \mathbf{H}_0 \cos^{-2}\phi$, where ϕ is the tilt angle and \mathbf{H}_0 is the field position for $\phi = 0$.

In addition to the primary RFSE series observed by KW in the $\mathbf{J} \perp \mathbf{H}$ polarization, we have observed other series of harmonically related signals when \mathbf{H} is tilted out of the sample plane. These signals are produced by different groups of electrons which are refocused at particular depths in the metal by their motion about \mathbf{H} . Each such series moves to increasing field with increasing tilt angle but with distinct tilt dependences. These features are illustrated in Fig. 1 which presents data taken for various tilt angles at a frequency of 33.694 MHz on a 0.116-mm-thick specimen of potassium at 1.4°K.

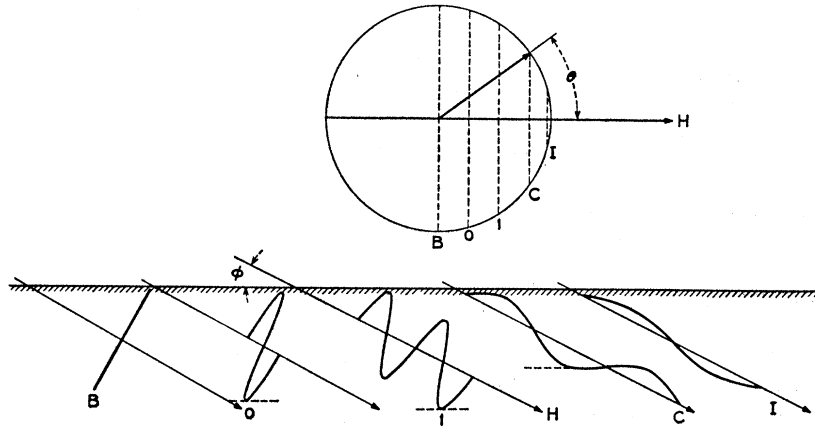
With currents polarized parallel to the projection of \mathbf{H} on the sample surface ($\mathbf{J} \parallel \mathbf{H}$) signals produced by

electrons in the vicinity of the limiting point are observed when \mathbf{H} is tilted a few degrees ($\gtrsim 7^\circ$) out of the sample plane. These signals are due to the transition from effective to ineffective orbits spanning the sample as the tilt angle is varied. In this polarization we also observe signals from the same groups of refocused electrons that produce the various signal series observed in the $\mathbf{J} \perp \mathbf{H}$ polarization.

For $H \gtrsim 3$ kG and $f \sim 30$ MHz, the sharp resistance anomalies of the fundamental size effect series give way to essentially sinusoidal oscillations of the same periodicity in \mathbf{H} . The oscillations appear in both polarizations but exhibit a cutoff which is very sensitive to tilt for the $\mathbf{J} \perp \mathbf{H}$ polarization. This cutoff occurs when the orbits of the effective electrons become so small that no net velocity is acquired by the electrons passing through the skin depth.

All of the signals enumerated above move to increasing magnetic field with tilt and are produced by electrons which are excited by a single passage through the fields in the skin depth. It is experimentally clear that the percentage change of the total surface impedance due to the signals is extremely modest for all cases and, since the driving currents are not significantly perturbed, a self-consistent calculation of the surface impedance is not required to understand the spectroscopic details of the RFSE anomalies. The picture which emerges is that of a weak but highly structured current distribution in the bulk of the metal which gives rise to impedance anomalies on interacting with the driving currents at the opposite surface. To determine the field position of the impedance anomalies we therefore examine the distance between "effective points" (segments of the electron's trajectory at which the velocity

FIG. 2. Projection of various orbits on the plane defined by \mathbf{H} and the sample normal \hat{n} when \mathbf{H} is inclined at an angle φ relative to the sample surface. Orbit B represents belly electrons at $\theta = \frac{1}{2}\pi$ on the Fermi surface which have no drift velocity along \mathbf{H} . Orbit 0 represents electrons refocused after $\sim \frac{1}{2}$ orbit about \mathbf{H} . These electrons produce the primary size effect series in the tilted field geometry. Orbit 1 represents electrons refocused after $\sim \frac{3}{2}$ orbits; these electrons produce a signal independent of the group 0 electrons. Orbit C (stair-step orbit) occurs at the transition from effective to ineffective orbits ($\theta_e = \varphi$ for a spherical Fermi surface). Orbit I has no point along its trajectory at which $\mathbf{v} \cdot \hat{n} = 0$ and is ineffective.



is parallel to the surface) of electron orbits from all regions of the Fermi surface.

IV. GEOMETRICAL MODEL

In this section we describe a mechanism which accounts for each of the signals observed in the RFSE experiments. The mechanism relies on current discontinuities produced by the electrons which go deepest into the metal between two zeros of normal velocity. In some cases many electrons from a considerable area of the Fermi surface travel to very nearly the same depth in the metal between two zeros of normal velocity to give a large contribution to the bulk current distribution and efficiently propagate the surface excitation several orbital diameters into the metal. Quantitatively we must determine the distribution of effective electrons as a function of their depth in the metal. We therefore present a straightforward calculation of the electron trajectories in the presence of a magnetic field tilted at an arbitrary angle relative to the sample surface. No attempt is made to solve the boundary-value problem. The model is therefore not self-consistent but it has the merit that it provides a quantitative description of the field position of the observed signals and identifies the position on the Fermi surface of the electrons which produce each signal. Signal line shapes and intensities must presumably wait upon the self-consistent solution of the boundary-value problem.

Since the actual fraction of the conduction electrons that participate in the RFSE phenomenon at any tilt angle is small, we assume that a well-defined skin depth $\delta \sim 10^{-4}$ cm is maintained by the "background" electrons and that the energy carried into the bulk of the metal by a specific group of electrons to produce a current sheet weakly affects the skin depth. Furthermore, since $\omega\tau \ll 1$, an electron which experiences fields of a particular phase will undergo a collision before the phase of the exciting currents has changed significantly. Finally, for $\omega_e\tau \gtrsim 1$ and $\omega \ll \omega_e$ all electrons whose trajectories will carry them through the skin depth within one orbit about the magnetic field will experience rf fields of the same phase. We may therefore treat the

problem as if there were a current sheet that is constant in time and localized within a depth δ of the sample surface and look for spatial variations of the current carried into the metal by the orbital motion of the electrons.

Proceeding in this manner we examine the trajectories of electrons at an angle θ on the Fermi surface in the presence of an external magnetic field \mathbf{H} inclined at an angle φ relative to the sample surface. The projections of various orbits on the plane defined by \hat{n} , the normal to the surface, and \mathbf{H} are sketched in Fig. 2. Only electrons which have $\mathbf{v} \cdot \hat{n} = 0$ in the skin depth are effective in carrying currents into the bulk of the metal (e.g., orbits B, 0, 1, and C in Fig. 2; orbit I is ineffective). To obtain the current distribution in the metal we must determine the *maximum* depth normal to the surface that an electron at an angle θ on the Fermi surface can traverse between two *adjacent* zeros of normal velocity ($\mathbf{v} \cdot \hat{n}$). This is the segment of the electron trajectory responsible for the *fundamental* size-effect signal as well as the *primary* size effect series. For $\omega_e\tau \gg 1$, one must also consider the depths attained successive complete orbits later. These depths are illustrated for an arbitrary orbit in Fig. 3. The depth d_n between relevant zeros of normal velocity is

$$d_n = \frac{2v_{\perp}}{\omega_e} \cos \varphi \cos \left[\sin^{-1} \left(\frac{v_{\parallel}}{v_{\perp}} \tan \varphi \right) \right] + \frac{2v_{\parallel}}{\omega_e} \sin \varphi \left\{ \left(n + \frac{1}{2} \right) \pi + \sin^{-1} \left(\frac{v_{\parallel}}{v_{\perp}} \tan \varphi \right) \right\},$$

$$n = 0, 1, 2, \dots \quad (1)$$

where v_{\perp} and v_{\parallel} are the components of \mathbf{v}_F perpendicular and parallel to the magnetic field. Equation (1) differs from that given by Koch and Wagner [Eq. (3) of Ref. 2]. Their expression does not take into account the fact that the relevant points on an orbit are zeros of normal velocity and that these zeros are *not* in general separated by exactly one-half of an orbit.

Physically, Eq. (1) is composed of two contributions. The first term is the projection of the orbit diameter

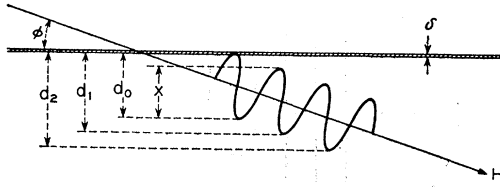


FIG. 3. Projection of an arbitrary orbit illustrating the notation used in the text.

onto the normal to the surface; the second term is the projection onto this same normal of the distance that the electron drifts between the two zeros of normal velocity. Equation (1) is independent of the geometry of the Fermi surface, being valid for any Fermi surface which has rotational symmetry about \mathbf{H} . For a spherical Fermi surface d_n reduces to

$$d_n = (2v_F/\omega_c) \left\{ \cos\varphi \sin\theta \cos[\sin^{-1}(\tan\varphi \cot\theta)] + \sin\varphi \cos\theta \left[(n + \frac{1}{2})\pi + \sin^{-1}(\tan\varphi \cot\theta) \right] \right\}, \quad (2)$$

where v_F is the Fermi velocity and θ is the polar angle on the Fermi surface measured from the magnetic-field direction as in Fig. 2.

For the sake of clarity, we will discuss the $n=0$ case in detail. The $n=1, 2, \dots$ cases are completely analogous to this case. For $n=0$, Eq. (2) becomes

$$d_0 = (2\hbar k_{Fc}/eH) \left\{ \cos\varphi \sin\theta \cos[\sin^{-1}(\tan\varphi \cot\theta)] + \sin\varphi \cos\theta \left[\frac{1}{2}\pi + \sin^{-1}(\tan\varphi \cot\theta) \right] \right\}. \quad (3)$$

This is the maximum depth that an electron can attain between two adjacent zeros of normal velocity. Only for $\tan\varphi \cot\theta \leq 1$ are electrons effective; for $\tan\varphi \cot\theta > 1$, the electrons have no point on their trajectory where $\mathbf{v} \cdot \hat{n} = 0$ and are ineffective.

Equation (3) is plotted for tilt angles of 0° and 15° in Fig. 4. Comparing the depth distribution of electrons for these two tilt angles reveals two important features. First, when the field is tilted relative to the sample plane a large number of electrons go deeper into the metal than the stationary ($\theta = \frac{1}{2}\pi$) electrons. For $\varphi = 15^\circ$, the maximum depth $d_{0 \text{ max}}$ is attained by electrons at $\theta_0 \sim 67^\circ$; furthermore, electrons from a wide band ($\Delta\theta \sim 15^\circ$) attain very nearly this same depth (refocusing). Second, there is a cutoff of coupling at a particular (tilt-dependent) angle θ_c on the Fermi surface in the tilted-field geometry which is not present at $\varphi = 0$. For a spherical Fermi surface $\theta_c = \varphi$.

The broad maximum in d_0 shown in Fig. 4 implies that many electrons which have their velocity in the skin depth parallel to the surface will arrive at very nearly the same depth in the metal when their velocity is again parallel to the surface. These electrons may be said to be refocused²³ by the magnetic field. The refocusing

²³ The refocusing mechanism discussed here is not to be confused with the refocusing mechanism presented by Azbel' (Ref. 3) for the field-parallel case. We are considering the motion of electrons on the Fermi surface in the presence of only a magnetic field and have not included the small perturbation on this motion due to the incremental velocity change experienced by the electrons on passing through the skin depth.

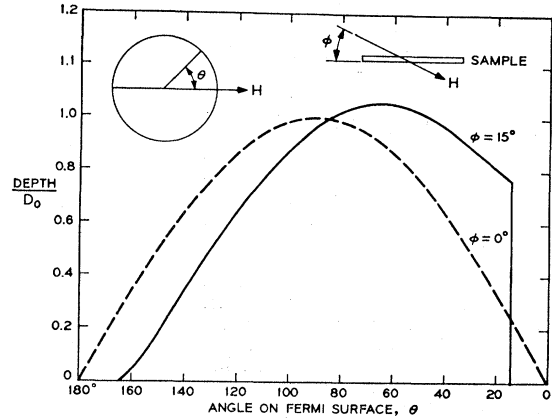


FIG. 4. Plot of d_0 versus θ for tilt angles of 0° (dashed curve) and 15° (solid curve). The maximum centered at $\theta \sim 67^\circ$ for $\varphi = 15^\circ$ produces the primary size effect series in the tilted field geometry. The discontinuity at $\theta_c = 15^\circ$ for $\varphi = 15^\circ$ is produced by the transition from effective to ineffective orbits.

mechanism arises because near the angle θ providing the maximum value of d_0 a slight increase in θ produces an increase in the orbit diameter and a decrease in drift velocity along \mathbf{H} . This broad maximum in $d_0(\theta)$ is a general characteristic of the tilted geometry. As φ is increased, the maximum moves deeper into the metal and is produced by electrons nearer the tip of the Fermi surface. These refocused electrons, rather than the stationary-orbit electrons proposed by Kaner,¹¹ produce the primary size effect series in the tilted geometry. Essentially, the band of stationary-orbit electrons is too narrow to dominate the current versus depth distribution despite the $\omega_c\tau$ enhancement.

The dependence of the field position of the fundamental size-effect signal on the tilt angle is readily determined. We note that in the limit $\delta/R \ll 1$ the RFSE measures *discontinuities* in the current distribution as they interact with the driving fields at the opposite surface of the specimen. When the field is parallel to the surface a discontinuity exists at a depth $d = D_0$, the orbit diameter of the belly electrons. The onset of the fundamental signal therefore occurs when D_0 is equal to the sample thickness L . In the tilted geometry a discontinuity appears at the maximum value of d_0 and the onset of the fundamental signal occurs at the magnetic field for which $d_0 = L$. Refocusing of electrons by their motion about the magnetic field in the tilted geometry is of little consequence for the fundamental size effect signal which is produced by the discontinuity and changes only slightly in line shape and intensity with tilt. However, the refocusing is efficient in propagating the surface excitation deep into the metal.

So far we have been concerned only with electrons which refocus after approximately one-half an orbit about \mathbf{H} . In the case of $\omega_c\tau \gg 1$ one must also consider subsequent zeros of normal velocity. The depths at which these zeros occur are given by Eq. (2) for $n=1, 2, 3, \dots$. The maxima of $d_n(\theta)$ for a given φ give rise to higher-

order singularities in the bulk current distribution. It is important to note that electrons for each value of n are refocused independently at a distinct depth $d_{n \max}(\theta)$ and produce distinct size-effect signals. This is in direct disagreement with the model of Koch and Wagner² in which it was assumed that the fundamental RFSE signal itself resulted from the superposition of currents carried by electrons coming from distinct zones on the Fermi surface after $\frac{1}{2}, \frac{3}{2}, \frac{5}{2}, \dots$ cyclotron orbits. In fact, distinct size effect series result from different sets of zeros of the normal velocity. It should also be recognized that in view of the reexcitation which occurs in the bulk of the sample one not only expects several distinct harmonically related series but also all possible combinations of such signals. It should therefore be clear that under long mean free path conditions even a simple spherical Fermi surface will produce enormously complicated RFSE spectra in a tilted field geometry.

Signals corresponding to a larger n value are produced by electrons at a smaller angle θ_n on the Fermi surface for a given φ . As φ increases the value of θ_n at $d_{n \max}$ moves rapidly toward θ_c . For $\theta_n > \theta_c$, the refocused electrons become ineffective and the current sheets disappear. As in the $n=0$ case, the tilt dependence of the $n=1, 2, \dots$ signals can be calculated in a straightforward manner assuming these signals are produced by the current discontinuity at the maximum value of d_n . The predicted tilt dependence for $n=0, 1$, and 2 is shown in Fig. 5.

One discontinuity evident in Fig. 4 remains to be discussed; this is the cutoff in coupling that occurs at θ_c when \mathbf{H} is tilted relative to the sample surface. The

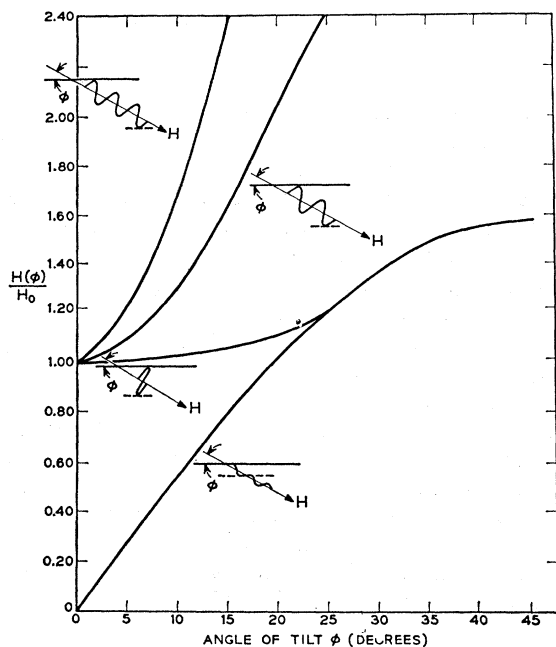


FIG. 5. Predicted tilt dependence for signals from $n=0, 1$, and 2 electrons and from the discontinuity at C.

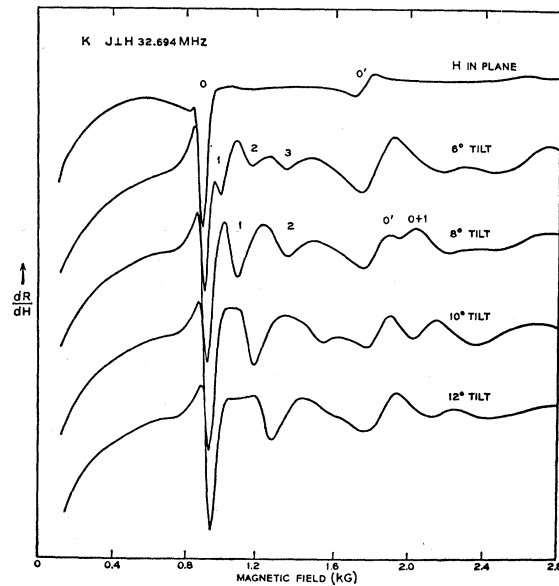


FIG. 6. Data taken on the same sample as those shown in Fig. 1. These data show the fundamental size effect signal (0) and its second harmonic ($0'$). When \mathbf{H} is tilted out of the sample plane (lower 4 traces) signals from electrons refocused after $\sim \frac{1}{2}$ (labeled 1), $\sim \frac{3}{2}$ (labeled 2), and $\sim \frac{5}{2}$ (labeled 3) orbits are observed. Signals produced by combinations of currents sheets are also observed (e.g., $0+1$).

transition from effective to ineffective orbits produces a current discontinuity of a completely different nature than either the deepest electrons for $\varphi=0$ or the refocused electrons for small tilt. There is no refocusing associated with the discontinuity at θ_c . Electrons following a trajectory such as C in Fig. 2 have a long path parallel to the surface. At slightly smaller values of θ (e.g., trajectory I in Fig. 2) there is no point on the orbit for which $\mathbf{v} \cdot \hat{n} = 0$.

A signal is observed from the transition between ineffective and effective electrons spanning the sample and provides an orbit caliper for electrons at the angle θ_c on the Fermi surface. Since θ_c is very small at small tilt angles, this allows one to measure orbits near the limiting point region of the Fermi surface. The tilt dependence of the field value at which this discontinuity reaches the opposite sample surface is also given by Eq. (2). This is obtained by setting $n=0$ and $\tan \varphi \cot \theta = 1$, which defines the cutoff. The resulting equation for d_c is

$$d_c = (2\pi \hbar k_{Fc} / eH) \sin \theta \cos \theta. \quad (4)$$

Equation (4) gives curve C of Fig. 5.

V. DISCUSSION

In this section we present data taken in potassium and make quantitative comparison between these data and the model of Sec. IV. Although the magnetic field position of any observed structure is independent of the driving current polarization, the two polarizations emphasize different regions of the Fermi surface.

Currents polarized perpendicular to \mathbf{H} are coupled most strongly to electrons near $\theta = \frac{1}{2}\pi$ on the Fermi surface, whereas currents parallel to \mathbf{H} couple most strongly to electrons near the limiting points. The two polarizations are therefore discussed separately.

A. $\mathbf{J} \perp \mathbf{H}$ Polarization

Data taken with the rf currents transverse to the magnetic field at 1.4°K and 32.694 MHz are shown in Fig. 6. The upper trace is the signal observed with \mathbf{H} accurately in the sample plane of a 0.116-mm-thick specimen. The fundamental size-effect signal at 846 G results from one extremal orbit diameter spanning the sample thickness. It was pointed out above that the low-field edge of the line was the point to be used to caliper the orbit diameter. Experimental studies of the frequency dependence of the fundamental signal demonstrate that the low-field edge of the line is also the only frequency-invariant point (see also Refs. 2 and 24). The over-all width of the fundamental signal proves to be proportional to $\omega^{-1/3}$ and is therefore proportional to the penetration depth δ of the driving electromagnetic fields,

$$2\delta/L \cong \Delta H/H. \quad (5)$$

While this provides a measurement of the rf penetration depth, the relation of δ to the number δ_0 obtained from anomalous-skin-effect calculations⁴ is not at all clear. δ_0 defined from the surface impedance gives only the ratio of the electric field to its normal derivative at the surface and does not directly yield the actual penetration depth of the fields. Line-shape calculations by Kaner and Fal'ko²⁰ indicate that the value of δ measured by the RFSE is expected to be $\sim (3-4)\delta_0$. In any event, δ is a characteristic parameter of the experiment and our data yield $\delta \cong (5-6)\delta_0$. Evidence will be presented below that δ is nearly constant over a large range of magnetic field and tilt angle.

The lower traces of Fig. 6 illustrate the effect of tipping the magnetic field out of the sample plane. As \mathbf{H} is canted relative to the sample surface the intensity of the higher-order impedance anomalies of the primary RFSE signal increase significantly. These anomalies have the same period as the fundamental RFSE signal and are produced by electrons reexcited in current sheets formed in the bulk by electrons from the vicinity of $\theta_{0 \max}$ on the Fermi surface. Azbel⁸ and Kaner¹¹ have shown that the excitation propagated by an "orbit chain" of this nature is weakly attenuated as long as the width of the current sheets is much less than their separation. While the increase in intensity of the higher-order signals is evidence of this enhanced penetration, the current sheets are not produced by stationary electrons as Kaner¹¹ proposed but rather by the drifting electrons which give rise to the fundamental RFSE signal. The fundamental signal itself is essentially un-

²⁴ A. Fukumoto and M. W. P. Strandberg, Phys. Letters 23, 200 (1966).

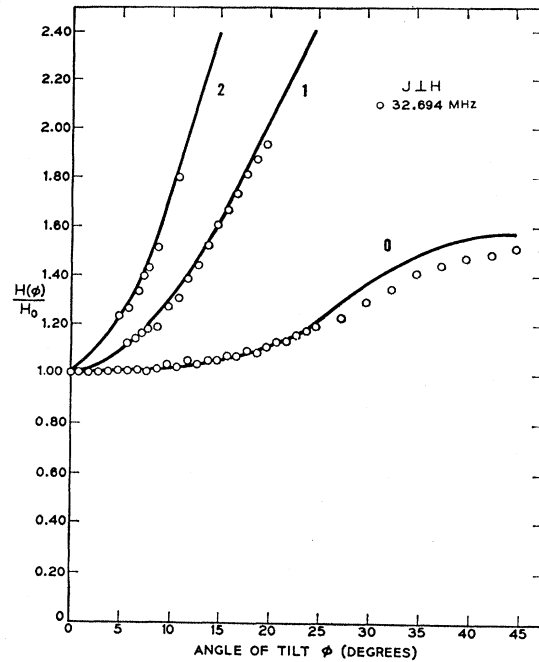


FIG. 7. Comparison of the experimental tilt dependence for $\mathbf{J} \perp \mathbf{H}$ (points) with the calculated tilt dependence. The deviation from the calculated curves for $\varphi \gtrsim 25^\circ$ presumably arises from the radical line shape change that occurs when the group C electrons merge with the 0 electrons.

changed in amplitude since it is produced by the current discontinuity from electrons at $\theta_{0 \max}$ on the Fermi surface and does not rely on secondary excitation of electrons in the bulk.

As φ is increased, signals produced by refocusing of the $n=1, 2,$ and 3 electrons emerge from the fundamental size-effect signal and move rapidly to increasing field with increasing tilt. These signals are independent of the primary size-effect series and are produced by electrons from different regions of the Fermi surface. At $H > 2H_0$ higher-order signals occur from secondary excitation of electrons by the current sheets produced by refocused $n=1, 2, \dots$ electrons. However, due to the finite mean free path of the electrons, these signals are strongly attenuated compared to $n=0$ signals. Thus the combination signal due to $d_{0 \max} + d_{1 \max} = L$ is clearly visible as indicated in Fig. 6 but $2d_{1 \max} = L$ yields only a very weak anomaly.

In Fig. 7 the tilt dependence observed for $\mathbf{J} \perp \mathbf{H}$ is compared with the dependence predicted by the geometrical model. For this comparison we have plotted the ratio of the onset of each line to the onset of the fundamental signal at $\varphi=0$. The agreement is good. The apparent disagreement for $\varphi \gtrsim 25^\circ$ results from the line shape change which occurs as the coupling cutoff rather than the refocusing discontinuity dominates the bulk current distribution. The functional form of the observed tilt dependence agrees with the model predictions, however.

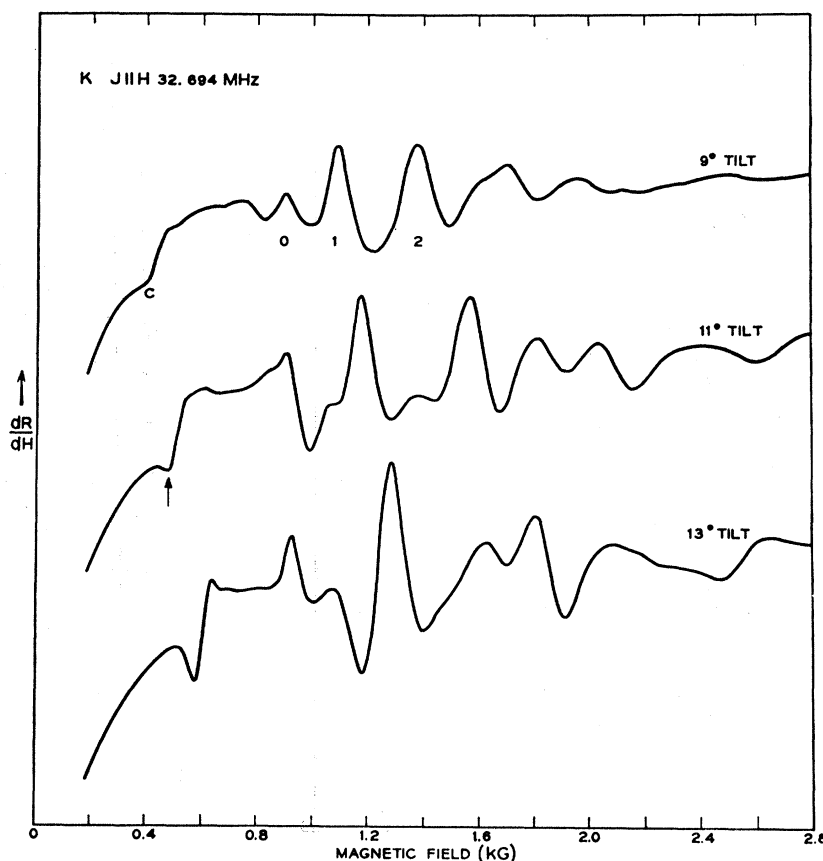


FIG. 8. Data taken with $\mathbf{J} \parallel \mathbf{H}$ on the same sample as those shown in Figs. 1 and 6 illustrating the signal observed at tilt angles of 9° , 11° , and 13° . Signals from electrons refocused after $\sim \frac{1}{2}$ orbit (0), $\frac{2}{3}$ orbits (1) and $\frac{3}{2}$ orbits (2) are observed in this polarization as well as in the $\mathbf{J} \perp \mathbf{H}$ polarization. In addition, a signal from the coupling cutoff at C is also observed for $\varphi \gtrsim 7^\circ$.

B. $\mathbf{J} \parallel \mathbf{H}$ Polarization

Data taken on the same sample and at the same frequency as those displayed in Figs. 1 and 6 are illustrated for currents parallel to the projection of \mathbf{H} on the sample plane in Fig. 8. When \mathbf{H} is in the sample plane the signal is very weak since the only current discontinuity is produced by electrons near $\theta = \frac{1}{2}\pi$ on the Fermi surface and these electrons are very weakly coupled to the rf currents. However, the intensity of the signals increases dramatically as \mathbf{H} is tilted out of the sample plane, and signals produced by each group of refocused electrons are apparent.

In this polarization the higher-order ($n=1, 2$) signals are more intense than the fundamental ($n=0$) signal. This intensity variation is opposite to that for the $\mathbf{J} \perp \mathbf{H}$ polarization and occurs because electrons which produce signals of successively larger n values are closer to $\theta=0$ on the Fermi surface and are therefore coupled more strongly to the exciting currents than the $n=0$ electrons.

In addition to the signals from refocused electrons, in this polarization signals are also observed from the coupling cutoff, the sudden transition from effective to ineffective orbits at $\theta_c = \varphi$. This signal is evident for $\varphi \gtrsim 7^\circ$ and is labeled C in Fig. 8. When $\mathbf{H} < \mathbf{H}_c$ the only electrons capable of completing an orbit in the specimen are ineffective. Suddenly, at $\mathbf{H} = \mathbf{H}_c$, effective electrons

can complete an orbit inside the specimen and are strongly coupled to the surface currents in both skin layers.

At $\varphi \sim 23^\circ$ the signal from the coupling cutoff merges with the signal from the refocused $n=0$ electrons. Data taken as these signals come together are shown in Fig. 9 where traces taken at tilt angles between 18° and 36° are presented. The tilt angle as well as the magnetic-field position at which these signals merge is in excellent agreement with the geometric model and provides added confirmation that one can determine precisely the region on the Fermi surface which produces each signal.

At larger tilt angles ($\varphi > 25^\circ$) effective electrons are no longer refocused. The observed size-effect signals are then produced entirely by the "stair-step" orbit at $\theta_c = \varphi$ (see Fig. 2). The line shape reverses in this region (Fig. 9). This reversal may be qualitatively understood as follows: At small tilt angles the majority of the effective electrons attain a depth greater than the depth d_c attained by electrons at θ_c . At $\varphi > 23^\circ$, the maximum depth attained by effective electrons in one orbit about \mathbf{H} is d_c . However, the signals continue to extend to a large magnetic field since secondary excitation in the bulk of the specimen is not required. As a result, the line shape of the higher-order signals is similar to that of the fundamental signal of this series. The transition from signals produced by effective electrons to signals

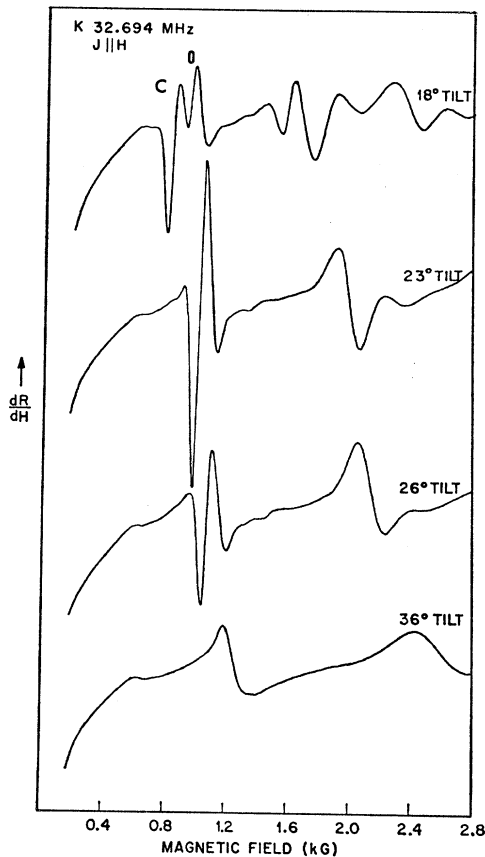


FIG. 9. Data taken with $\mathbf{J} \parallel \mathbf{H}$, showing the region in which the signal from the coupling cutoff C merges with the electrons refocused after $\sim \frac{1}{2}$ orbit (0). At 23° tilt the two signals have almost completely merged. By $\varphi = 36^\circ$ the structure is completely determined by electrons at θ_c .

produced by ineffective electrons in the tilted geometry has also been studied very recently in Cd by Neberezhnykh and Maryakhin.¹⁹

In Fig. 10 we compare the experimental observations for $\mathbf{J} \parallel \mathbf{H}$ with the predicted curves of Fig. 5. For the 0, 1, 2 curves the maxima of the dR/dH signals (normalized to the onset of the fundamental signal for $\mathbf{J} \perp \mathbf{H}$ at $\varphi = 0$) are plotted to remove any ambiguities about the position of the onset of the lines. This maximum is the most prominent feature of the lines and could be most accurately determined. Therefore, only the functional dependence of the 0, 1, and 2 curves should be compared with the calculations. The data of curve C were plotted using the onset of the line (arrow, Fig. 8). The over-all agreement between the experimental data and the predictions of the model is felt to be quite satisfactory.

Recently there has been some controversy as to whether the Fermi surface of potassium is accurately spherical or somewhat distorted in the vicinity of the limiting point due to a lack of complete periodicity of the metal as in a spin-density-wave²⁵ or charge-density-

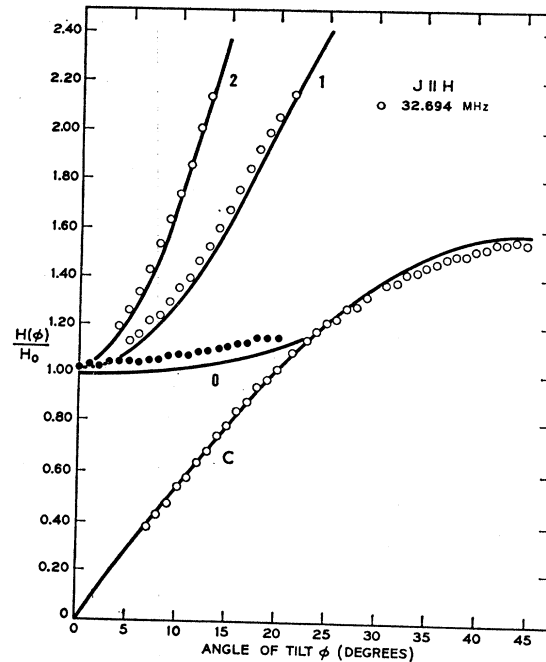


FIG. 10. Comparison of the experimental tilt dependence for $\mathbf{J} \parallel \mathbf{H}$ (points) with the calculated tilt dependence. The maxima of the lines (normalized to the onset of the signal for $\mathbf{J} \perp \mathbf{H}$ at $\varphi = 0$) are plotted for curves 0, 1, and 2. The low-field minima (see arrow, Fig. 8) of curve C is plotted.

wave ground state.²⁶ The proposed "lemon-like" distortion would reduce the maximum value of v_{11} from v_F ($v_F = 0.71 \times 10^8$ cm/sec)²² to 0.56×10^8 cm/sec.²⁷ The resulting v_1 would never vanish. Therefore, if the Fermi surface were lemon-shaped with the unique axis along \mathbf{H} ²⁸ a signal from the limiting-point electrons would be observed for $\varphi = 0$. This signal would be more intense than any signal observed for $\mathbf{J} \parallel \mathbf{H}$ and would occur at $\mathbf{H}/H_0 \approx 0.6$ for $\varphi = 0$. An increase in φ would result in the signal moving slowly to increasing field and intercepting curve C of Fig. 10 at $\varphi \sim 25^\circ$. Conversely signal C of Fig. 8 would not exist. The agreement of not only the field positions of all the observed signals but also the angular position at which the various signals coalesce with the behavior calculated for a spherical Fermi surface graphically demonstrate that the Fermi surface of potassium is not appreciably distorted by a spin or charge density wave at the magnetic fields of these experiments. This is in agreement with the observations of Koch and Wagner.²

In a recent discussion of conduction-electron spin-resonance spectra in potassium samples prepared and

²⁶ A. W. Overhauser, Bull. Am. Phys. Soc. 13, 42 (1968); and (to be published).

²⁷ We have used the effective mass obtained from cyclotron resonance by Grimes and Kip (Ref. 10) to evaluate v since the experiments are at low frequency compared to the phonon frequency. The value of $v_{H \max}$ for the spin density wave model is obtained from Eq. (23) of Ref. 28.

²⁸ A. W. Overhauser and S. Rodriguez, Phys. Rev. 141, 431 (1966).

²⁵ A. W. Overhauser, Phys. Rev. Letters 13, 190 (1964).

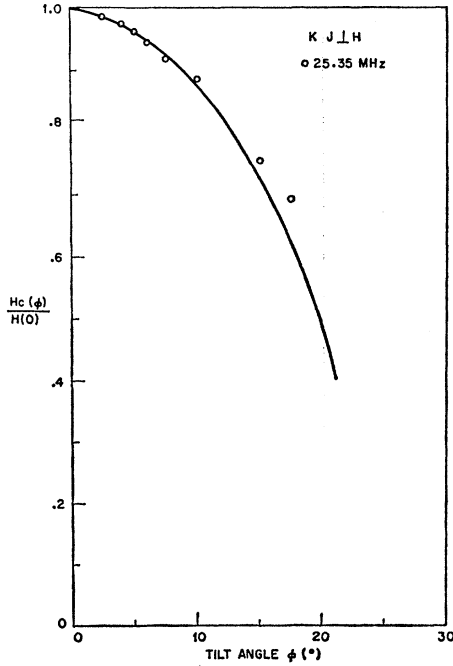


FIG. 11. Comparison of the angular dependence of the cutoff of the sinusoidal variations with the calculated dependence for $\mathbf{J} \parallel \mathbf{H}$. The data are normalized to the curve at $\varphi = 2.5^\circ$.

handled exactly as are those of our RFSE experiments,²⁹ Overhauser and deGraaf³⁰ are led to suggest that such samples are inhomogeneous in that sections are strain free and that in these sections the “lemon” axis is aligned parallel to \mathbf{H} and that other sections are strained and have the lemon axis oriented perpendicular to the sample surface. Our failure to observe *any* RFSE signal near $\mathbf{H}/\mathbf{H}_0 \approx 0.6$ for $\varphi = 0$ strongly implies that this more complicated picture cannot be correct.

C. Oscillatory Signal

When the magnetic field is in the plane of the sample the intensity of the size-effect signals decreases very rapidly with increasing magnetic field for both polarizations. However, if \mathbf{H} is inclined relative to the surface the signals are observed to extend to much larger values of magnetic field due to enhanced current penetration into the bulk of the metal. After four or five current sheets are formed in the metal the widths of the current sheets become comparable to their spacing and the surface impedance variations become sinusoidal in character. These variations have the same periodicity as the fundamental signal since signals from $n = 1, 2, \dots$ electrons are strongly attenuated due to the finite mean free path.

In the $\mathbf{J} \perp \mathbf{H}$ polarization the sinusoidal oscillations exhibit a high-field cutoff whose position is a strong

function of tilt. The magnetic-field value at which these oscillations disappear for a given tilt angle also decreases with the experimental frequency approximately as $\omega^{1/3}$ over the frequency range from 2–35 MHz. The cutoff occurs when the orbit diameter becomes so contracted that no net excitation is obtained by refocused $n = 0$ electrons as they pass through the skin-effect region. The field position of this cutoff is given by the geometrical model as follows: As H increases the *minimum* distance x (Fig. 3) between two adjacent zeros of $\mathbf{v} \cdot \hat{n}$ decreases. For a spherical Fermi surface x is readily calculated and is given by

$$x = (2\hbar k_{FC}/eH) \{ \cos \varphi \sin \theta \cos[\sin^{-1}(\tan \varphi \cot \theta)] - \sin \varphi \cos \theta [\frac{1}{2}\pi - \sin^{-1}(\tan \varphi \cot \theta)] \}. \quad (6)$$

When $x < \delta$ the electron has two zeros of normal velocity (and therefore two positions of maximum excitation) in the skin depth. However, with $\mathbf{J} \perp \mathbf{H}$, if $\mathbf{E}_t \cdot \mathbf{v}$ is positive for one excitation it must be negative for the other. Any velocity obtained at the first “stopping point” is given up at the second stopping point and little or no net excitation is carried into the bulk of the metal. The cutoff for the $\mathbf{J} \perp \mathbf{H}$ polarization is therefore given by

$$H_x = (2\hbar k_{FC}/e\delta) \{ \cos \varphi \sin \theta \cos[\sin^{-1}(\tan \varphi \cot \theta)] - \sin \varphi \cos \theta [\frac{1}{2}\pi - \sin^{-1}(\tan \varphi \cot \theta)] \}. \quad (7)$$

Since the value of θ for the $n = 0$ signal is known (Sec. IV), one can immediately plot the tilt dependence of the cutoff. In Fig. 11 we compare the observed cutoff field with Eq. (7). The data were normalized to the theoretical curve at $\varphi = 2.5^\circ$ which corresponds to measuring the penetration depth at this field and tilt angle. The value obtained for δ is $\sim 10\%$ greater than the value of δ obtained from measurement of the linewidth of the fundamental size-effect signal. The agreement of the data with the calculated curve over the entire angular range for which the oscillations persist indicates that the skin depth is essentially constant, at least for $\varphi \lesssim 20^\circ$. This is in agreement with observations of the fundamental size-effect linewidth which is also constant for $\varphi \lesssim 20^\circ$.

Finally, the model predicts that the sinusoidal oscillations should not suffer a cutoff of this type for $\mathbf{J} \parallel \mathbf{H}$. Even though the electrons have two points of maximum interaction in the skin depth, $\mathbf{E} \cdot \mathbf{v}$ has the same sign for both excitations when $\mathbf{J} \parallel \mathbf{H}$. Therefore the electrons can receive a net velocity increment from the surface currents even when $x < \delta$. To illustrate that this is indeed the case Fig. 12 shows data taken for $\mathbf{J} \parallel \mathbf{H}$ at tilt angles of 20° and 30° . Although at this frequency the oscillations have disappeared by tilt angles of 20° for $\mathbf{J} \perp \mathbf{H}$, they are seen to extend to fields greater than 13 kG even at $\varphi = 30^\circ$ for $\mathbf{J} \parallel \mathbf{H}$. The signal becomes weaker as the widths of the current sheets exceed their separation but they do not exhibit a sharp cutoff for this polarization.

²⁹ W. M. Walsh, Jr., L. W. Rupp, Jr., and P. H. Schmidt, Phys. Rev. 142, 414 (1966).

³⁰ A. M. deGraaf and A. W. Overhauser, Bull. Am. Phys. Soc. 13, 42 (1968); and (to be published).

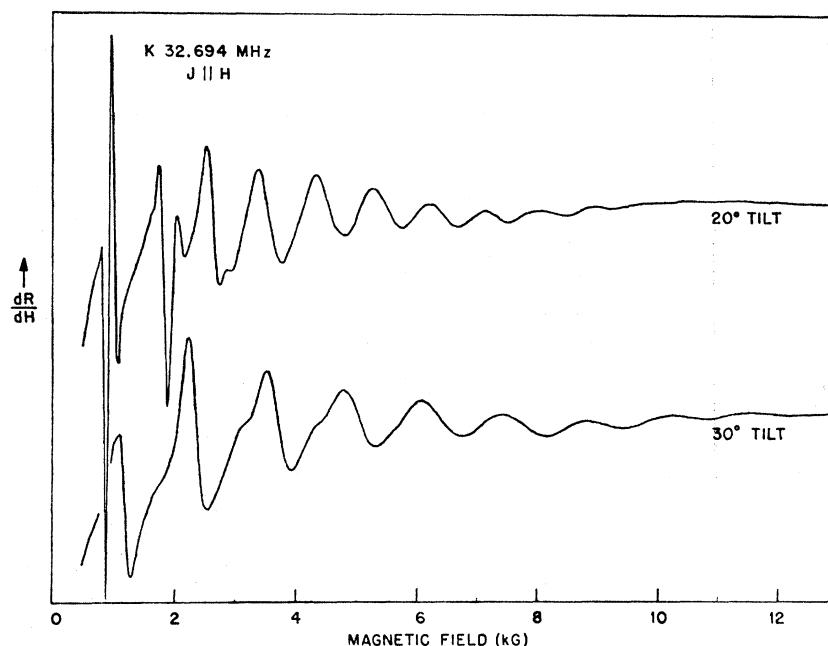


FIG. 12. Data taken from 0–13 kG with $J \parallel H$ at tilt angles of 20° and 30° . These data were taken on the same sample as those shown in Fig. 1 and illustrate the existence of the sinusoidal signals at high fields and large tilt angles for this polarization.

VI. SUMMARY

These measurements on potassium, whose spherical Fermi surface greatly simplifies the orbit geometries, illustrate the value of the RFSE for making precise Fermi-surface measurements. Most experiments emphasize extremal dimensions of the Fermi surface. However, the ability to measure orbit dimensions over large regions of the Fermi surface by the size-effect technique is demonstrated in the measurements of H_c discussed in Sec. V B.

Although the size-effect experiments are performed under anomalous skin-effect conditions which are mathematically complex, the surface fields and currents are only slightly perturbed by the effect. Therefore, the data can be evaluated in a geometric manner which avoids the theoretical complications inherent in a self-consistent solution of the boundary-value problem while providing a physical understanding of the effect. While this has been demonstrated only for a spherical Fermi surface, Eq. (1) which gives the field position for each signal observed is general for any surface with cylindrical symmetry about the magnetic field. The spirit of the geometrical model considerably simplifies the problem of considering such experiments in more complicated cases.

Finally, we note that size-effect signals with the field normal to the surface have been observed in Sn at radio

frequencies by Gantmakher and Kaner³¹ and in Ga in dc measurements by Munarin and Marcus.³² Calculations by Gantmakher and Kaner³¹ indicate that this effect should be present for a spherical Fermi surface, even though it is produced entirely by ineffective electrons. No field normal signal was observed in the course of our experiments. However, Libchaber³³ has recently observed a very weak field normal signal in potassium using the rf transmission technique reported by Walsh and Grimes.⁸ Related signals have also been observed by Schultz and Dunifer at microwave frequencies.³⁴

ACKNOWLEDGMENTS

Our original interest in the RFSE phenomenon was stimulated by Dr. C. C. Grimes whose advice and criticism have been of great value. We have also benefited from discussions with Dr. P. M. Platzman, Dr. P. A. Wolff, and Dr. K. B. Jefferts. We are particularly indebted to Dr. G. A. Baraff for several discussions concerning the geometrical model.

³¹ V. F. Gantmakher and E. A. Kaner, *Zh. Eksperim. i Teor. Fiz.* 48, 1572 (1965) [English transl.: *Soviet Phys.—JETP* 21, 1053 (1965)].

³² J. A. Munarin and J. A. Marcus, in *Proceedings of the Ninth International Conference on Low-Temperature Physics, Columbus, Ohio*, edited by J. A. Daunt *et al.* (Plenum Press, Inc., New York, 1965).

³³ A. Libchaber (private communication).

³⁴ S. Schutz (private communication).